Published in final edited form as:
Virology. 2013 December ; 447(0): 312–325. doi:10.1016/j.virol.2013.09.020.

Retargeting of Gene Expression Using Endothelium Specific Hexon Modified Adenoviral Vector

Sergey A. Kaliberov[1], **Lyudmila N. Kaliberova**[1], **Zhi Hong Lu**[2], **Meredith A. Preuss**[3], **Justin A. Barnes**[4], **Cecil R. Stockard**[4], **William E. Grizzle**[4], **Jeffrey M. Arbeit**[2], and **David T. Curiel**[1]

[1] Department of Radiation Oncology, School of Medicine, Washington University in St. Louis, St. Louis, Missouri, United States of America

[2] Department of Surgery, School of Medicine, Washington University in St. Louis, St. Louis, Missouri, United States of America

[3] Department of Medicine, University of Alabama at Birmingham, Birmingham, Alabama, United States of America

[4] Department of Pathology, University of Alabama at Birmingham, Birmingham, Alabama, United States of America.

Abstract

Adenovirus serotype 5 (Ad5) vectors are well suited for gene therapy. However, tissue-selective transduction by systemically administered Ad5-based vectors is confounded by viral particle sequestration in the liver. Hexon-modified Ad5 expressing reporter gene under transcriptional control by the immediate/early cytomegalovirus (CMV) or the Roundabout 4 receptor (Robo4) enhancer/promoter were characterized by growth in cell culture, stability *in vitro*, gene transfer in the presence of human coagulation factor X, and biodistribution in mice. The obtained data demonstrate the utility of the Robo4 promoter in an Ad5 vector context. Substitution of the hypervariable region 7 (HVR7) of the Ad5 hexon with HVR7 from Ad serotype 3 resulted in decreased liver tropism and dramatically altered biodistribution of gene expression. The results of these studies suggest that the combination of liver detargeting using a genetic modification of hexon with an endothelium-specific transcriptional control element produces an additive effect in the improvement of Ad5 biodistribution.

Keywords

adenovirus; targeting; endothelium; Roundabout 4 promoter; hexon

Sergey A. Kaliberovskaliberov@wustl.edu**Lyudmila N. Kaliberova**lkaliberova@wustl.edu**Zhi Hong Lu**luz@wudosis.wustl.edu**Meredith A. Preuss**mpreuss@uab.edu**Justin A. Barnes**barnesja@uab.edu**Cecil R. Stockard**stockard@uab.edu**William E. Grizzle**wgrizzle@uab.edu**Jeffrey M. Arbeit**arbeitj@wustl.edu**David T. Curiel**dcuriel@wustl.edu.

Introduction

Currently, adenoviral (Ad) vectors are widely used as gene delivery vehicles. Development of efficient and selective gene therapy vectors will increase the efficacy and safety of gene-based therapeutics. In this regard, human adenovirus serotype 5 (Ad5) vectors are well suited to gene therapy because they exhibit a favorable safety profile, have a high transgene capacity, *in vivo* stability, low oncogenic potential, and are readily amenable to tropism modification cell type specific vector targeting. However, predominant liver transduction limits the utility of Ad5-based vectors for gene therapy applications. Thus, a major goal in Ad5 mediated gene delivery is to overcome the natural tropism of Ad5 for the liver and to optimize tissue-specific targeting. Transcriptional targeting of Ad5 using tissue-specific promoters can redirect or eliminate liver transgene expression, potentially mitigating hepatotoxicity and increasing vector safety profiles.

The endothelium plays a critical role in cancer development as well as in many inflammatory and cardiovascular diseases. As such, the endothelium has become an important aim for gene therapy interventions for a wide range of diseases (Aird, 2003). In this regard, targeted endothelial cell delivery is crucial for effective Ad-mediated gene therapy. Adenoviral vector transcriptional endothelial cell targeting has been reported using a number of promoters, including flt-1 (Reynolds et al., 2001), flk-1 (Savontaus et al., 2002), pre-proendothelin-1 (Greenberger et al., 2004), VEGFR2 (Song et al., 2005), Tie2 (Cefai et al., 2005), ICAM-1 (Wung, Ni, and Wang, 2005), KDR (Yang et al., 2006) and VEGF (Takayama et al., 2007). The majority of these studies focused on the utility of the promoter to target proliferating endothelium in cancer therapy applications. Although this approach has allowed an improvement in target cell-to-liver gene delivery ratios, the performance of these endothelial-specific promoters has been suboptimal due to the low-level transgene expression. In this study we are particularly interested in the employment of the Roundabout 4 receptor (Robo4) promoter for endothelial-specific gene targeting. The existing data of Robo4 expression and function has been controversial. In general, the proposed functions of Robo4 can be divided into two categories: pro-migratory/pro-angiogenic functions, as well as an anti-migratory stabilization of the existing vasculature (reviewed in (Zhuang et al., 2011)). Initial studies demonstrated that Robo4 is a transmembrane receptor of the roundabout gene family that is expressed in endothelium, where it is believed to play a role in migration and/or angiogenesis (Huminiecki et al., 2002) as well as in hematopoietic stem cells and in lymphatic endothelial cells (Smith-Berdan et al., 2011; Zhang et al., 2012). Robo4 has been shown to have a role in vascular development (Kaur et al., 2006), angiogenesis (Bedell et al., 2005), and to be upregulated in patients with idiopathic pulmonary arterial hypertension (Edgar et al., 2006). The 3-kb fragment of the Robo4 promoter was shown to direct endothelial cell-specific expression in the embryonic and adult vasculature of Hprt locus-targeted mice (Okada et al., 2007). It has been shown that Robo4 expression causes a migratory response of endothelial cells to Slit and activation of Robo4 by Slit2 inhibits vascular endothelial growth factor mediated endothelial cell spreading, migration and tube formation (Park et al., 2003; Seth et al., 2005). Slit2-mediated effects in the vasculature and mammary gland are Robo4-dependent and result in stabilization of the vascular network (Jones et al., 2008; Jones et al., 2009; Marlow et al., 2010). However, there is no evidence for direct binding of Slit2 to Robo4, and Slit2 is not the only known ligand for the Robo4 receptor (Koch et al., 2011). In general, these features support the utilization of the Robo4 promoter as a transcriptional targeting tool for subsets of endothelial cells.

The major pathway of liver transduction involves interactions of Ad capsid proteins with circulating blood cells and with plasma proteins including several components of complement pathway and blood coagulation zymogens. Recent studies have revealed that

liver uptake of Ad5 is mediated by a high-affinity interaction between the major protein in the Ad5 capsid, hexon, and γ-carboxylated glutamic acid (Gla) domain of coagulation factor X (FX). The Ad5-FX complex attaches to hepatocytes through the binding of the serine protease domain of FX to cell surface heparan sulfate proteoglycans (HSPGs) (Parker et al., 2006; Shayakhmetov et al., 2005; Zinn et al., 2004). Early studies determined that liver transduction by Ad5 in mice can be abolished by pretreatment with drugs that block coagulation, such as warfarin or snake venom protein X-bp. Treatment of mice with warfarin, which depletes FX, significantly reduced Ad5 liver transduction. Also, it was shown that different Ad serotypes interact with FX with distinct affinities. For instance, Ad serotypes 26, 35 and 48 bind to FX with relatively low affinity compared to Ad5 (Kalyuzhniy et al., 2008; Waddington et al., 2008) (Parker et al., 2006) (Parker et al., 2007). More recently, it was shown that ablation of FX binding to Ads with modified hexon protein resulted in decreased liver tropism (Alba et al., 2010; Alba et al., 2009; Short et al., 2010).

Our experiments sought to test the efficacy of the combination of endothelial-specific gene expression with mitigated hepatic sequestration of hexon-modified Ads. We developed a panel of hexon-modified Ad5 vectors including Ads expressing reporter transgenes under transcriptional control of a 3.0-kb fragment of the Robo4 enhancer/promoter (Okada et al., 2007). Substitution of the Ad5 hexon with the hypervariable region 7 (HVR7) from Ad serotype 3 (Ad3) hexon resulted in decreased liver tropism and improved biodistribution of gene expression following Ad systemic administration. The combination of liver detargeting using a genetic modification of the hexon with a transcriptional targeting approach using endothelium-specific Robo4 promoter could be used in the future to treat diseases with significant endothelium involvement.

Results

Recombinant adenoviral vectors

For this study we have developed a series of recombinant Ad5-based vectors expressing reporter transgenes under transcriptional control of the ubiquitous CMV or endothelial-specific Robo4 promoter (Table 1). AdH5*7*CMVLuc vector contains point mutations within HVR5 (T270P and E271G) and HVR7 (I421G, T423N, E424S, L426Y, and E451Q) of the Ad5 hexon protein, resulting in the substitution of HVR5 and HVR7 with sequences from Ad serotype 26 (Alba et al., 2009). AdH3CMVLuc hexon protein contained the first 55 amino acid residues (aa) of Ad5 hexon, followed by Ad3 hexon sequence, and then the last 45 aa of Ad5 hexon. This resulted in the replacement of Ad5 hexon between amino acids 54 and 907 with Ad3 hexon sequence. Since the N-terminal (aa 1 to 53) and C-terminal (aa 908 to 952) regions are highly conserved between the hexon proteins of Ad5 and Ad3 (only 5 and 2 aa are different in the two regions, respectively), the resultant hexon gene is 99.3% identical to the native Ad3 hexon gene (Wu et al., 2002). We have developed novel AdH5/H3CMVLuc and AdH5/H3RoboLuc vectors encoding hexon chimeras with substitution from 382 to 588 aa of Ad5 hexon with a 206 aa fragment that included HVR7 from Ad3 hexon. AdH5CMVLuc and AdH5RoboLuc vectors expressing wild-type hexon were used as isogenic control vectors.

Robo4 promoter activity in vitro

For initial evaluation of the ability of the Robo4 promoter to drive cell-specific gene expression in the context of an Ad5 vector containing wild-type hexon, human endothelial HCAEC and HPAEC and mouse endothelial SVEC4-10 cells were infected with AdH5CMVLuc or AdH5RoboLuc, encoding the firefly luciferase (Luc) gene under control of the CMV or Robo4 promoter, respectively. Forty-eight hours after infection, cells were harvested and Luc expression was analyzed using the luciferase assay system. Levels of Luc

expression varied in different cell lines (Fig. 1A) in proportion to viral doses of infection (results not shown). Infection with AdH5RoboLuc yielded lower Luc expression in comparison with AdH5CMVLuc and levels of Luc expression of endothelial cells were correlated with Robo4 mRNA expression (data not shown).

Robo4 expression in vivo

Transcriptional activity of cell-specific promoters typically correlates with the level of expression of the corresponding endogenous gene. We hypothesized that the activity of the Robo4 promoter would correlate to the relative levels of Robo4 mRNA expression and the relative percentage of vascular endothelial cells in each organ. We determined endogenous Robo4 mRNA expression in liver, spleen, lung, kidney and heart using quantitative RT-PCR. Lung and spleen demonstrated high levels of Robo4 mRNA expression (21- and 25-fold ($P<0.05$), respectively) in comparison with liver, whereas kidney and heart showed the lowest levels of Robo4 mRNA expression (Fig. 1B).

Biodistribution of Luc expression

To evaluate Ad-mediated Luc expression *in vivo*, liver, spleen, and lung were collected at 3 days after systemic administration of AdH5RoboLuc or AdH5CMVLuc. As shown in Fig. 1C, AdH5CMVLuc-mediated expression was observed mainly in the liver and spleen with relatively low expression in the lung following *i.v*. injection. Luciferase expression in the liver of AdH5RoboLuc-injected mice was 255-fold lower than following AdH5CMVLuc injection (Fig. 1C) with maintenance of levels Luc expression in lung and spleen. Despite of high levels of Robo4 mRNA expression in lung tissues (Fig. 1B), biodistribution study revealed that the absolute levels of Luc expression in the liver remain higher in comparison with lung following AdH5RoboLuc injection. However, the utilization of the Robo4 rather than the CMV promoter produced 227-fold increase in the lung-to-liver and a 3,280-fold increase in the spleen-to-liver ratios of Luc expression compared to AdH5CMVLuc (Fig. 1D).

Immunohistochemistry

To verify the activity of the Robo4 promoter *in vivo*, we employed AdH5CMVCEA and AdH5RoboCEA vectors encoding a truncated form of human carcinoembryonic antigen (CEA) as we have previously described (Everts et al., 2005). As illustrated in Fig. E, in the lung, both the CMV and Robo4 promoters directed CEA expression in endothelial cells of both microvessels and large blood vessels (Fig. 1E, lower panels). However, AdH5RoboCEA produced more evenly distributed, darker staining in the microvascular endothelium compared with AdH5CMVCEA (Fig. 1E, lower panels). In the liver, AdH5CMVCEA-injected mice demonstrated CEA expression in Kupffer cells and hepatocytes (Fig. 1E, upper left panel), whereas CEA staining was undetectable in the livers of mice receiving AdH5RoboCEA, (Fig. 1E, upper right panel).

To identify cell type in the lung that was transcriptionally targeted by the Robo4 promoter, hCAR transgenic mice were injected *via* tail vein with AdH5RoboEGFP. Two days post injection mouse lungs were collected and immunofluorescent EGFP expression localization was analyzed. As shown in Fig. 1F, EGFP expression in lung tissue was co-localized with the endothelial cell markers CD31 and endomucin. Collectively these data revealed that the elevated reporter gene expression in the lung was due to endothelial cell specific expression of under transcriptional control of the Robo4 promoter. In contrast, in liver and spleen (data not shown) the CMV-driven transgene expression targeted hepatocytes and reticuloendothelial cells.

In vivo gene transfer blocking assay

To investigate whether blocking FX Ad5 hexon binding can decrease liver uptake and subsequently enhance AdH5Robo4Luc-mediated gene transfer, we examined the effect of preincubation of Ad5 vectors with tF10, a truncated form of hFX lacking the serine protease domain necessary to bridge the Ad5 to HSPGs, but retain Gla domain essential for Ad5 binding. As shown in Fig. 2A and 2B, preincubation of AdH5CMVLuc and AdH5RoboLuc with tF10 resulted in decreased transgene expression in the liver and increased Luc expression in the lung, and significantly improved the lung-to-liver (L/L) ratio, 12- and more than 16-fold, respectively ($P < 0.05$), compare to mock-treated Ads (Fig. 2C).

Thus, the combination of liver detargeting using ablation of the FX interaction with hexon and a transcriptional targeting using Robo4 promoter can improve Ad-mediated gene expression in the lung endothelium. Rather than modulate FX binding by using tF10 blocking protein, we created a panel of genetically engineered hexon-modified Ads, including Ad vectors expressing Luc under control of the Robo4 promoter (Table 1).

The one-step growth curve

Since hexon is the most abundant protein in the Ad capsid, we evaluated whether hexon modification changes viral replication in cell culture and stability *in vitro*. To compare replication of Ads with various modifications in the hexon protein, HEK293 cells were harvested at different times after infection with AdH5CMVLuc, AdH5/H3CMVLuc, AdH5*7*CMVLuc and AdH3CMVLuc, and subjected to $TCID_{50}$ assay. As shown in Fig. 3A, viral replication of hexon-modified Ads was decreased over 100-fold for AdH3CMVLuc and ~10-fold for AdH5/H3CMVLuc or AdH5*7*CMVLuc compared to AdH5CMVLuc vector with wild-type hexon.

Thermostability of hexon-modified Ads

Next, we tested how modifications in the hexon protein affect the structural integrity of the Ad virion by comparing the thermostability of hexon-modified vectors to AdH5CMVLuc. Based on results of preliminary study that demonstrated temperature-dependent decreasing of Ad-mediated gene transfer, the viruses were preincubated at 42°C for different times before the infection of A549 cells, and relative gene transfer efficiency was obtained by comparing with the gene transfer of unheated Ads. As shown in Fig. 3B, gene transfer efficiency of AdH5CMVLuc, AdH5/H3CMVLuc and AdH5*7*CMVLuc was not significantly reduced following a 30-min incubation, and about 50% of Luc expression was retained even after a 60-min incubation at 42°C. In contrast, gene transfer efficiency of AdH3CMVLuc was reduced by more than 80% following the first 30-min incubation and more than 100-fold after a 60-min incubation at 42°C.

Modification of the Ad5 hexon decrease hFX-mediated Ad transduction in vitro

Because all tested Ads contain identical wide-type fiber protein, we investigated whether modifications of Ad5 hexon alter FX binding and subsequent Ad-mediated gene transfer *in vitro*. To evaluate the effect of preincubation of AdH5CMVLuc, AdH5/H3CMVLuc, AdH5*7*CMVLuc and AdH3CMVLuc with hFX in transduction of Luc expression was measured 48 hours following infection of hepatocellular carcinoma HepG2 and human liver epithelial THLE-3 cells compared to cells infected with control PBS-treated Ad (Fig. 3C). Infection with AdH5CMVLuc produced significantly increased transgene expression in HepG2 and THLE-3 cells, 5.4- and 2.8-fold, respectively, when preincubated with hFX, relative to PBS-treated Ad. In contrast, hexon-modified Ads demonstrated negligible change in transduction following hFX preincubation.

Distribution of reporter gene expression in vivo

To evaluate biodistribution of Ad-mediated Luc expression in C57BL/6 mice, liver, spleen, and lung were harvested after systemic administration of hexon-modified AdH5/H3CMVLuc, AdH5*7*CMVLuc or AdH3CMVLuc, or AdH5CMVLuc vectors. To produce the pharmacological blockage of Ad5 sequestration in the liver, mice were injected with the anti-coagulant drug warfarin, which decreases levels of circulating vitamin-K dependent coagulation factors, including FX (Koski et al., 2009; Shashkova et al., 2008; Short et al., 2010). AdH5CMVLuc was administered either alone or following pretreatment with warfarin 3, and 1 day prior to Ad injections (Fig. 4A, AdH5cmvLuc + W). Three days after vector administration Luc activity was measured in organ lysates. As shown in Fig. 4A, Luc expression was observed mainly in the liver and spleen with relatively low expression observed in the lung following systemic AdH5CMVLuc administration. Treatment with warfarin before AdH5CMVLuc injection resulted in 67-fold reduction ($P<0.01$) in Luc expression in the liver and more than 15-fold increase ($P<0.05$) in the lung compared with AdH5CMVLuc alone. Luciferase expression in the liver was significantly lower after injection with AdH5/H3CMVLuc, AdH5*7*CMVLuc, and AdH3CMVLuc in 361-, 34- and 7-fold, respectively, compared to AdH5CMVLuc. There were no significant differences across Luc expression in the spleen after injection of AdH5CMVLuc plus warfarin, AdH5/H3CMVLuc, AdH5*7*CMVLuc or AdH3CMVLuc in comparison with AdH5CMVLuc. As illustrated in Fig. 4A, differing levels of Luc expression were detected in the lung after systemic administration of the various Ad vectors.

Treatment with warfarin before AdH5CMVLuc injection resulted in 882- ($P<0.001$) and 37-fold ($P<0.01$) increases in the lung-to-liver and spleen-to-liver ratio of Luc expression, respectively, in comparison with AdH5CMVLuc alone (Fig. 4B). The lung-to-liver ratio was significantly increased 1,177-, 19- and 141-fold following injection with AdH5/H3CMVLuc, AdH5*7*CMVLuc and AdH3CMVLuc vectors, respectively, compared to AdH5CMVLuc. Also, AdH5/H3CMVLuc, AdH5*7*CMVLuc, and AdH3CMVLuc injection had increased spleen-to-liver ratios (176- ($P<0.01$), 25- ($P<0.01$) and 5-fold ($P=0.06$), respectively), in comparison with AdH5CMVLuc.

Biodistribution of hexon-modified endothelium targeted Ad vectors

Despite the advantages of hexon-modified vectors in liver detargeting, the efficacy of recombinant Ads for gene delivery to the endothelium of mice has been limited. We hypothesized that gene transfer to the endothelium could be enhanced by combining liver detargeting with Robo4-mediated transcriptional targeting. Systemic administration of AdH5/H3CMVLuc, AdH5RoboLuc, and AdH5/H3RoboLuc in C57BL6J mice produced Luc expression in the liver that was 59-, 431-, and over 240,000-fold, respectively, lower than AdH5CMVLuc (Fig. 5A). Luciferase expression in the spleen was 36-fold higher with AdH5RoboLuc than AdH5CMVLuc ($P<0.05$).

As shown in Fig. 5B, the lung-to-liver ratio was significantly increased after administration of AdH5/H3CMVLuc, AdH5RoboLuc, and AdH5/H3RoboLuc (258-, 167-, and more than 92,000-fold, respectively) compared to AdH5CMVLuc. The lung-to-liver ratio was increased in mice injected with AdH5RoboLuc (167-fold; $P<0.01$) compared to AdH5CMVLuc and after AdH5/H3RoboLuc injection (475-fold; $P<0.001$) in comparison with AdH5/H3CMVLuc. The spleen-to-liver ratio was significantly increased following injection with AdH5/H3CMVLuc, AdH5RoboLuc, and AdH5/H3RoboLuc by 110-, 11,200-, and over 108,000-fold, respectively, compared to AdH5CMVLuc. The spleen-to-liver ratio was significantly increased by 11,200-fold after AdH5RoboLuc injection in comparison with AdH5CMVLuc and by 980-fold following AdH5/H3RoboLuc injection compared to AdH5/H3CMVLuc.

Quantitative analysis of the Ad hexon gene expression

To confirm distribution of viral particles *in vivo*, number of Ad hexon gene copies was measured by quantitative PCR in organs at 24 hours following *i.v*. injection with AdH5RoboLuc and AdH5/H3RoboLuc (Fig. 5C). The lung-to-liver ratio of Ad hexon gene copy numbers was increased in mice injected with hexon-modified AdH5/H3RoboLuc vector (19-fold; $P<0.05$) compared to AdH5RoboLuc with wild-type Ad5 hexon. In contrast, the spleen-to-liver ratio of Ad hexon gene copy numbers was increased 7-fold following injection with hexon-modified vector in comparison with AdH5RoboLuc.

To investigate whether modification in Ad5 hexon can decrease the liver toxicity and activation of systemic inflammation mice were injected *via* tail vein with AdH5/H3RoboLuc or AdH5RoboLuc. As shown in Fig. 5D-F, levels of enzymatic activity of ALT and AST were significantly higher in mice injected with AdH5RoboLuc displaying wild-type hexon comparison with PBS and AdH5/H3RoboLuc. It is well known that Kupffer cell uptake of Ad5 leads to an innate immune response characterized by the release of proinflammatory cytokines such as interleukin-6 (IL-6) (Sharma et al., 2010). Thus, based on observations that Ads with hexon modification have reduced sequestration in the liver, compared with wild-type Ad5, we next measured IL-6 levels in the serum at 24 hours after virus administration. AdH5/H3RoboLuc-mediated induction of serum IL-6 was significantly reduced after intravenous injection, compared with mice injected with an equivalent dose of AdH5RoboLuc with wild-type hexon ($P<0.05$; Fig. 5F).

Biodistribution in the hCAR transgenic mice

As endothelial cells have negligible levels of expression of human Ad5 primary receptor, and to isolate transcription as a single experimental variable for proof of concept experiments we tested our Ad vectors in transgenic mice ubiquitously expressing hCAR. As illustrated in Fig. 6A, AdH5RoboLuc and AdH5/H3RoboLuc injection produced 240- and 1,450-fold less ($P<0.001$) Luc expression in the liver compared to AdH5CMVLuc, respectively, and AdH5/H3CMVLuc-mediated Luc expression was only slightly reduced (4-fold) compared to control vector. There were no significant differences across Luc expression in tested organs except in the spleen, and Luc expression after AdH5/H3CMVLuc injection was increased (8-fold; $P<0.05$) in comparison with AdH5CMVLuc.

As shown in Fig. 6B, the lung-to-liver ratio was slightly increased in mice injected with AdH5/H3CMVLuc (~4-fold), and significantly increased following AdH5RoboLuc (73-fold), and AdH5/H3RoboLuc (over 250-fold) injection in comparison with AdH5CMVLuc. The spleen-to-liver ratio of Luc expression was significantly increased after AdH5RoboLuc injection (331-fold) compared to AdH5CMVLuc and following AdH5/H3RoboLuc injection (105-fold) in comparison with AdH5/H3CMVLuc.

To further compare viral genome levels *in vivo* after single tail vein injection of AdH5RoboLuc or AdH5/H3RoboLuc we have evaluated Ad hexon gene expression in organs of mice by quantitative PCR. As shown in Fig. 6C, absolute numbers of Ad genomes in liver following injection with AdH5/H3RoboLuc were decreased compare to AdH5RoboLuc at 24 hours post-injection that resulted in increased lung-to-liver and spleen-to-liver ratios (7- and 5-fold, respectively).

Additionally, we have evaluated the liver toxicity and activation of systemic inflammation following systemic administration of wild-type and hexon-modified Ads, mice were injected *via* tail vein with AdH5RoboLuc and AdH5/H3RoboLuc. Serum ALT, AST and IL-6 levels in mice injected with AdH5RoboLuc were significantly higher in comparison with PBS-treated animals (Fig. 6 D-F). However, there were no significant differences across levels of

enzymatic activity of ALT and AST as well as IL-6 concentration in serum after injection mice with AdH5/H3RoboLuc compared to the PBS-treated group. Collectively the results of these studies suggest that the combination of liver detargeting using a genetic modification of the hexon protein with a transcriptional targeting approach using endothelium-specific Robo4 promoter would further improve the biodistribution of gene expression following systematical administration of Ad5-based recombinant vectors.

DISCUSSION

The tendency of *i.v.* administered Ad5 to localize in the liver represents a major factor limiting current strategies to accomplish Ad5-based vector targeting *via* a systemic delivery approach. In the first instance, the sequestration of a major administered fraction of viral particles in the liver limits availability for target cell transduction. In addition, Ad5 toxicities have been linked to vector effects within the liver. The fact that endothelium is the first cellular contact for systemically administered Ads, and that venous blood flow is first directed through the pulmonary vasculature, suggests that efficient targeting of cell types within the lung may preclude the need for Ad5 modifications that ablate liver sequestration mechanisms. Although most of the hexon sequence is highly conserved among Ad serotypes, several HVRs are known to exist within surface exposed loops, and these have been implicated in FX binding. Recently, hexon genetic modifications have been used to abolish Ad5 liver tropism; including modification of one or more of HVRs, addition of small peptides in the HVR, point mutations, or substitution of the Ad5 hexon with a hexon from different Ad serotypes. Ad5 hexon HVR5 and HVR7 are critical for the high-affinity hexon interaction with FX (Alba et al., 2009). FX cognate HVR domain modification regions produced profound biodistribution alterations, with decreased liver sequestration and greater splenic accumulation of Ad vectors (Alba et al., 2010; Alba et al., 2009).

In this study we have employed a series of Ad vectors with hexon modification to ablate viral particle association with serum FX and thereby mitigate liver sequestration. Whereas such approach allowed valid targeting gains in systemic delivery models, employment of a whole hexon chimera strategy was limited by virologic factors with suboptimal viral particle-to-infectivity ratios were associated with major alterations of capsid proteins (Wu et al., 2002). To address this issue we sought to modify the hexon of the parental Ad5 exclusively with Ad3 hexon domains that could abolish FX binding. In this regard, HVR7 of serotype 5 hexon has been shown to specifically interact with FX. On this basis, we replaced Ad5 HVR7 with the corresponding Ad3 hexon HVR7 domain.

As expected, all hexon-modified Ads produced negligible changes in gene transfer in representative liver cells *in vitro* following preincubation with hFX at physiological concentrations. However, the results obtained from the one-step Ad growth kinetics assay demonstrated decreased viral replication of hexon-modified Ads, most evident for the hexonchimeric AdH3CMVLuc, compared to AdH5CMVLuc with wild-type hexon. Additionally, gene transfer efficiency of AdH3CMVLuc was significantly reduced following incubation at 42°C in comparison with other tested Ads, suggesting reduced structural stability of this vector. These findings are in agreement with previous observations (Short et al., 2010; Wu et al., 2002) that the replacement of Ad5 hexon, the major capsid protein of the virion, with Ad3 serotype hexon protein dramatically reduces packaging of the Ad5 genome as well as stability of the virion, as compared to Ad5s with the native hexon or Ad5 hexon with Ad3 HVR7 substitution, or point mutations in HVR5 and HVR7.

Consistent with reports by others (Reynolds et al., 2001; Short et al., 2010), our experimental data provide evidence of relatively high levels of Ad5-mediated gene expression in the liver and spleen 3 days after *i.v.* administration. We have observed reduced

liver sequestration of hexon-modified Ads in all *in vivo* models compared to AdH5CMVLuc with wild-type hexon. A major disadvantage of C57BL6 mouse models for biodistribution studies has been that systemic administration of Ad5-based vectors resulted in preferential accumulation in the liver, with negligible transduction of other major organs, including the spleen, lung, kidney, brain, muscle and intestine. This property of Ad5-based vectors with wild-type capsid resulted in relatively low (between 10^{-5} - 10^{-4}) lung-to-liver ratios of gene expression for AdH5CMVLuc.

In this study it could be seen that the genetic capsid modification dramatically enhanced the lung-to-liver reporter gene expression ratio. Moreover, H5/H3 substitution accomplished liver untargeting at a level comparable to that achieved by our earlier full hexon serotype swap approach (Short et al., 2010). Importantly, the HVR7 substitution allowed for comparable gene transfer to cellular targets *in vivo* and was associated with improved vector virologic properties. However, real world translational applications demand sufficient selective gene expression in the context of endothelium cells. As a first approach to this challenge we exploited the utility of a combination of endothelial-specific targeting and mitigation of liver sequestration by using hexon-modified Ad5-based vectors. We created and tested a panel of Ad vectors with progressively increasing potential hepatocyte and liver reticuloendothelial system detargeting. Adenoviral vectors were constructed with the promiscuous CMV or the Robo4 endothelial-specific enhancer/promoter and with or without modified HVR7 to mitigate liver sequestration of the viral particles.

There are several approaches modify Ad5 tropism to accomplish the vascular endothelium targeting (Baker et al., 2005). The transductional targeting strategies seek to re-direct Ad5 binding to non-native receptors expressing on specific cell type. These approaches utilize Ad capsid display of peptides or bispecific antibodies cognate endothelial cell surface receptors (Glasgow, Everts, and Curiel, 2006; Kim et al., 2011; Preuss et al., 2008; Reynolds et al., 2001; Work et al., 2006) as well as Ad5 pseudotyping using fiber substitution with knob from different serotypes (Bachtarzi et al., 2011; Preuss et al., 2008; Shinozaki et al., 2006). Targeting of gene expression in the context of Ad employ can also be achieved with transcriptional targeting methods whereby transgenes are placed under the control of a tissue-specific promoter (Dong and Nor, 2009; Greenberger et al., 2004; Savontaus et al., 2002). Initial evaluation of the Robo4-driven Luc expression in endothelial cells *in vitro* demonstrated relatively low levels of promoter activity in comparison with AdH5CMVLuc. However, compared with other promoters tested to date (Cefai et al., 2005; Greenberger et al., 2004; Reynolds et al., 2001; Savontaus et al., 2002; Song et al., 2005; Takayama et al., 2007; Wung, Ni, and Wang, 2005; Yang et al., 2006), the Robo4 promoter displayed significantly less liver tropism and higher endothelial-specific expression *in vivo*. Remarkably, the lung endothelial expression was specific and high, while the liver expression was barely detectable by immunohistochemistry analysis. Direct analysis of lung tissue confirmed that the reporter gene expression was localized principally within the target cells of the pulmonary vascular endothelium. The use of Robo4-driven Luc-expressing Ads also allowed us to detect differences in the net gene expression in different organs. These two methods are complementary in their representation of promoter activity in this mouse model, with immunostaining allowing clear identification of cell types where the Robo4 promoter is active, and Luc allowing for sensitive quantification of promoter activity. These studies have confirmed that transcriptional targeting with the Robo4 enhancer/promoter allowed dramatic enhancement of vascular-specific gene delivery. In addition, adjunctive targeting strategies (hexon ablation) further enhanced the lung-to-liver ratios achieved *in vivo*.

Efficient Ad5 infection requires the expression of the hCAR for attachment and integrins for virus internalization. Human Ad5 uptake has still been shown to occur with low efficiency

in murine cells that lack hCAR, in part, due to murine CAR expression that allow infection by human Ad5 when transfected into CAR-negative cell lines (Bergelson et al., 1998) or by interaction between the penton base protein and integrins on the cell surface (Wickham et al., 1993). Since the endothelium is refractory to human Ad5 infection, we also chose to evaluate Robo4 promoter in transgenic hCAR mice, which ubiquitously express the primary attachment receptor for human Ad5. Using this model to facilitate Ad5 infection *in vivo* allows the study of promoter activity with Ad vectors while eliminating the variables introduced by varying susceptibility to Ad infectivity in different tissues (Tallone et al., 2001). We have previously reported increased lung localization of Ad in transgenic hCAR mice following systemic administration, demonstrating a marked increase in susceptibility of the pulmonary vasculature of these transgenic mice to Ad infection compared to wild-type C57BL6 mice (Everts et al., 2005). Building on this finding, we have evaluated Robo4-driven reporter gene expression *in vivo* using Ads with a genetic modification of the hexon protein. We have shown that utilization of the Robo4 promoter for transcriptional targeting in combination with H5/H3 modification can significantly improve the lung-to-liver ratio in comparison with AdH5CMVLuc, over 250-fold in transgenic hCAR mice injected with AdH5/H3RoboLuc, compared to slightly 4-fold increase following AdH5/H3CMVLuc, and increased by 73-fold ($P < 0.01$) after AdH5RoboLuc injection due to profound decrease in liver-associated expression. Collectively, the results of toxicity studies suggest that the combination of liver detargeting using a genetic modification of the hexon protein with a transcriptional targeting approach using endothelium-specific Robo4 promoter decrease the levels of enzymatic activity of ALT and AST as well as marker of systemic inflammation IL-6. Recent studies have shown that association Ad5 hexon with FX resulted in innate immunity activation (Doronin et al., 2012) as well as that Ad5-FX interaction protected from antibody- and complement-mediated neutralization in mice (Xu et al., 2013). The complexity of interaction Ad5 with the host resulted in only modest increasing in the absolute levels of Luc expression in the lung in comparison with profound decreasing of gene expression in the liver following systemic administration of hexon-modified Ad vectors.

The literature also suggests that the Robo4 promoter/enhancer may be useful in a cancer gene therapy context because of its role in angiogenesis and endothelial migration. We and others shown that Robo4 expression is markedly increased on the tumor-associated vasculature and provides the basis for specific of Ad-mediated Robo4-driven gene expression (Z.H. Lu et al., submitted) (Huminiecki et al., 2002) (Grone et al., 2006) (Seth et al., 2005) (Gorn et al., 2005) (Legg et al., 2008). Employment of the Robo4 promoter/enhancer for endothelium-specific transcriptional targeting of therapeutic gene expression is limited by relatively low activity in comparison with the CMV promoter. One of attractive approach to overcome this drawback is using the Robo4 promoter for targeted toxic/suicide gene therapy. The rationale behind targeted suicide gene therapy is that after specific expression of cytotoxic gene the systemic toxicity commonly associated with, and a major limitation of, conventional therapy is avoided. The construction of such vectors is under way in our laboratory. Thus, additional experiments that are beyond the scope of this study are required to evaluate employment of the Robo4 promoter for cancer gene therapy.

To our knowledge, this is the first report of the Robo4 promoter being utilized alone or in combination with hexon modification of Ad5 vector for liver untargeting. We have demonstrated that Ad5 vector tropism can be modified in order to give a “target tissue on” and “liver off” profile that can eventually enhance specificity of gene delivery. The results of these studies suggest that the combination of liver detargeting using a genetic modification of the hexon protein with a transcriptional targeting approach using endothelium-specific Robo4 promoter produces an additive effect in improving of biodistribution of Ad-mediated transgene expression in mice. In summary, these data

indicate that employing hexon modification and endothelial transcriptional targeting in combination provides a promising approach for gene therapy of diseases with significant endothelium involvement.

Materials and methods

Cells and reagents

The human hepatocellular carcinoma HepG2, human lung adenocarcinoma A549, transformed small vessel murine endothelial SVEC4-10 cells (all obtained from ATCC, Manassas, VA), and human embryonic kidney HEK293 (Microbix Biosystems, Ontario, Canada) cells were cultured in DMEM/F12 (Mediatech, Herndon, VA) containing 10% fetal bovine serum (FBS) (Summit Biotechnology, Fort Collins, CO). THLE-3 cells (human liver epithelial cells immortalized with SV40 large T antigen) were obtained from ATCC and were grown in BEGM growth media (Clonetics, Walkersville, MD). Primary human coronary artery endothelial cells (HCAEC) and pulmonary artery endothelial cells (HPAEC) were obtained from Cambrex (Baltimore, MD) and were cultured in Clonetics EC basal media (Cambrex) containing factors provided in the Singlequot Bullet Kit (Cambrex). All cells were cultured in a humidified atmosphere with 5% CO_2 at 37°C.

Purified human coagulation factor X (hFX) was obtained from Haematologic Technologies (Essex Junction, VT). Warfarin and peanut oil were purchased from Sigma-Aldrich (St. Louis, MO).

Adenoviral vectors

Replication incompetent *E1*- and *E3*-deleted Ad5 vectors were created using a two-plasmid rescue method. The plasmids encoded expression cassettes comprised of the human cytomegalovirus major immediate-early enhancer/promoter (CMV) or the Robo4 promoter coupled to either firefly luciferase (Luc), carcinoembryonic antigen (CEA) or enhanced green fluorescent protein (EGFP) transgenes, followed by the bovine growth hormone polyadenylation signal. These expression cassettes were cloned into a shuttle plasmid (pShuttle, Qbiogene, Carlsbad, CA) and confirmed by using restriction enzyme mapping and partial sequence analysis. The shuttle plasmids were linearized with *Pme* I and integrated into the Ad5 genome by homologous recombination with pAdEasy-1 plasmid in the *E. coli* strain BJ5183. The recombinant viral genomes were then transfected into HEK293 cells using SuperFect Transfection Reagent (Qiagen, Chatsworth, CA), where they were packaged into virus particles. To generate hexon-modified AdH5/H3CMVLuc and AdH5/H3RoboLuc vectors, the *SexA* I - *Hpa* I digest product of Ad5 hexon was substituted with a 618 bp fragment from Ad3 hexon (nucleotides 1127-1745). To create AdH3CMVLuc and AdH5*7*CMVLuc vectors, a 6710 bp *Sfi* I fragment (two unique *Sfi* I sites flank the hexon protein coding region) of Ad5 was substituted with a *Sfi* I fragment from pAd5/H3GL (provided by Dr. H. Wu, Tulane University, New Orleans, LA) and pAd5*7* (provided by Dr. A.H. Baker, University of Glasgow, Glasgow, UK) plasmids, respectively. The insert sequences were confirmed by partial sequencing analysis. Viruses were rescued and propagated in HEK293 cells and purified twice by CsCl gradient centrifugation and dialyzed against 10 mM HEPES, 1 mM $MgCl_2$, pH 7.8 with 10% glycerol as previously described (He et al., 1998). Viral titer was measured by a 50% tissue culture infectious dose ($TCID_{50}$) assay. Briefly, HEK293 cells were plated into 96-well tissue culture plates at 5×10^3 cells per well, and then serial dilutions of viral stock were added directly to the cells. Cells were incubated for 14 days, and relative cell density was determined using a crystal violet staining assay. Cell culture medium was removed and surviving cells were then fixed and stained with 2% (w/v) crystal violet (Sigma-Aldrich) in 70% ethanol for 3 hours at room temperature. The plates were extensively washed, air-dried, and optical density was

measured at 570 nm using a V Max plate reader (Molecular Devices Corporation, Sunnyvale, CA). The number of wells with observable cytopathic effect per each row was determined. The viral titer was calculated by the Karber equation: $T = 10^{1+D(S-0.5)} \times V^{-1}$, where T is infectious titer in $TCID_{50}$ ml^{-1}, D is the $\log_{10}$ of the dilution, S is the $\log_{10}$ for the initial dilution plus the sum of ratios, and V is the volume in ml of the diluted virus used for infection. Multiplicity of infection for subsequent experiments was expressed as $TCID_{50}$ per cell. Also, the concentration of viral particles (vp) was determined by measuring absorbance of the dissociated virus at A_{260} nm using a conversion factor of 1.1×10^{12} vp per absorbance unit.

Gene transfer in vitro

HCAEC, HCAEC and SVEC4-10 cells were seeded at 1×10^5 cells per well in 12-well tissue culture plates and allowed to grow overnight. The next day, cells were infected with 10 $TCID_{50}$ per cell in 0.2 ml per well in triplicate. After 1 hour, viral infection media was removed and fresh media was added. Forty-eight hours afterward, cell culture media was removed and cells were washed one time with PBS, cells were lysed and Luc activity was analyzed as described below.

Growth kinetics of Ad vectors

HEK293 cells were plated into 6-well tissue culture plates at 5×10^5 cells/well and allowed to adhere overnight. The next day, cells were infected with Ad vectors at 5 $TCID_{50}$ per cell in DMEM/F12 with 2% FBS for 1 hour, then culture medium was removed and fresh media containing 10% FBS was added to each well. Cells and culture medium were harvested at different times after infection, subjected to three freeze-thaw cycles, and after centrifugation supernatants were used for determination of viral titer by the $TCID_{50}$ assay.

Thermostability in vitro

A549 cells were plated in 24-well tissue culture plates in triplicate at a density of 5×10^4 cells/well, allowed to adhere and grow overnight. The next day, recombinant Ads were incubated at 42°C for different times then added to cells as described above. Forty-eight hours after infection cells were lysed and Luc activity was analyzed as described above. The relative infectivity was obtained by changing the relative light units (RLU) readings of the heat-treated viruses to the percentage of the readings of untreated viruses.

Gene transfer in presence of hFX

HepG2 and THLE-3 cells were seeded in 24-well tissue culture plates in triplicate at 5×10^4 cells/well. Next day, recombinant Ads were incubated for 1 hour with hFX at 8 μg/ml. Cells were infected with recombinant Ad vectors at 5 $TCID_{50}$ per cell as described above. Forty-eight h after infection, culture medium was removed, cells were washed with PBS, lysed and analyzed for Luc activity.

Luciferase assay

The Luciferase Assay System (Promega) and ORION microplate luminometer (Berthold Detection systems, Oak Ridge, TN) were used for the evaluation of Luc activity of infected cells. Luciferase activity was normalized by the protein concentration of the cell lysate using DC Protein Assay (Bio-Rad, Hercules, CA), according to the manufacturer's instructions. Data are expressed as relative light units (RLU) per 1×10^4 cells and bars represent the mean ± the standard deviation (s.d.).

In vivo studies

For *in vivo* experiments, 5-7 weeks old female C57BL6J mice were purchased from the Jackson Laboratory (Bar Harbor, ME). The transgenic female hCAR mice were a generous gift from Dr. S. Pettersson (Karolinska Institute, Sweden). The human coxsackie adenovirus receptor (hCAR) mice express a truncated receptor lacking the cytoplasmic domain necessary for signaling, but retain Ad5 binding, allowing Ad5 transduction of all organs in the animal under transcriptional control of the human ubiquitin-C promoter (Tallone et al., 2001). It was previously reported that hCAR mice had increased localization of Ad5 in the lungs following systemic administration compared to wild-type mice, demonstrating a marked increase in gene transfer to the pulmonary vasculature in these mice (Everts et al., 2005). This study was carried out in strict accordance with the recommendations in the Guide for the Care and Use of Laboratory Animals of the National Institutes of Health. Biodistribution studies were carried out according to the Institutional Animal Care and Use Committee (approved protocol # 20110035). All animals were housed under pathogen-free conditions according to the guidelines of the American Association for Accreditation of Laboratory Animal Care, with access to chow and water *ad libitum*. To produce pharmacological blockade of Ad5 binding to FX, C57BL/6 mice were pretreated with warfarin (5 mg per kg) dissolved in peanut oil and injected subcutaneously 3 days and 1 day prior to Ad injections. For each of the biodistribution experiments, mice were injected intravenously *via* the tail vein with 5×10^8 $TCID_{50}$ of recombinant Ad vectors. Three days after injection animals were humanely sacrificed by CO_2 inhalation, major organs were harvested and snap frozen in ethanol/dry ice mix and assessed for reporter gene expression using Luc assay. Briefly, tissues were lysed in reporter lysis buffer (Promega) and subjected to three freeze-thaw cycles to ensure complete lysis. Samples were centrifuged and supernatant analyzed for Luc activity using the Luciferase Assay System (Promega) as described above. Luciferase activity was normalized by the protein concentration of the cell lysate using DC Protein Assay (BioRad), according to the manufacturer's instructions. Data is expressed as relative light units (RLU) per mg of total protein and bars represent the mean ± the standard deviation (s.d.). Lung-to-liver and spleen-to-liver ratios were calculated for each individual animal with the RLU normalized by the protein concentration of the cell lysate and bars represent the mean ± s.d.

Immunohistochemistry analysis

Organs from mice were cut into 1-2 mm section and were fixed in neutral buffered 10% formalin for a minimum of 6 hours before paraffin embedding. Tissue sections were attached to microscope slides at 60°C for 2 hours and subsequently deparaffinized with 3 baths of xylene. The sections were rehydrated through graded ethanol baths from 100% to 70%. Three percent hydrogen peroxide was applied for 5 min followed by 3% goat serum for 20 min to block non-specific staining. Rabbit anti-carcinoembryonic antigen (CEA) antibody (Chemicon, Temecula, CA) diluted 1:1000 was applied at 25°C for 1 hour and rinsed with Tris buffer (0.05M Tris, 0.15M NaCl, 0.1% TritonX100, and pH 7.6). The secondary antibody (biotinylated goat anti-rabbit, Jackson Immuno Research Laboratories, West Grove, PA) and streptavidin-HRP (Signet Laboratories, Dedham, MA) were added for 20 min each with Tris buffer rinses between each step. The 3-3′-diaminobenzidine (BioGenex, San Ramon, CA) chromagen was applied to the sections for 7 min and the tissues were lightly counterstained with Mayer's Hematoxylin. Sections were then dehydrated through graded ethanol baths to xylene and cover slips mounted with Permount. Slides were analyzed in a blinded fashion and images shown are representative of 6 animals per group with the experiment performed twice. Images were acquired with a Nikon Optiphot-2 microscope (X600 – lens – Plan APO60/0.95, 900C, bright field of CEA antibody) using a SPOT 2 camera and software (the images are unmodified).

Co-immunofluorescence analysis

For analysis of immunofluorescent localization of EGFP reporter gene expression mouse lungs were collected, post-fixed in paraformaldehyde for 2 hours at room temperature, cryopreserved in 30% sucrose for 16 hours at 4°C, and embedded in NEG-50 compound using the 2-methylbutane/liquid nitrogen method. Sixteen-micrometer frozen sections were air-dried briefly, washed in PBS, blocked with protein block (1% donkey serum in PBS containing 0.1% Triton X-100) for 1 hour, and incubated with primary antibodies diluted in the protein block over night. Primary antibodies included rat anti-endomucin (1:1000, eBioscience), Armenian hamster anti-CD31 (1:1000, Millipore), and rabbit anti-GFP (1:400, Life Technologies). After washes with PBS, the slides were incubated with corresponding secondary antibodies conjugated with Alexa Fluor 488 and Alexa Fluor 594 (1:400; Jackson Immunologicals) and counterstained for nuclei with SlowFade Gold Antifade mounting reagent with 4′,6-diamidino-2-phenylindole (DAPI, Life Technologies). Fluorescence microscope images were collected using an Olympus Soft Imaging Solutions FVII digital camera with Extended Focal Imaging (EFI) function.

In vivo hFX blocking assay with tF10

We have developed the E1/E3-deleted Ad5tF10 vector encoding human tF10 gene corresponding to the truncated form of hFX (aa 1-128) under control of the CMV promoter element. The tF10 open reading frame (ORF) contained the first 128 aa of the hFX light chain, which includes a γ-carboxylated glutamic acid (Gla), and two epidermal growth factor-like (EGF_C, EGF_N) domains was amplified by PCR. To construct the pShuttletF10 plasmid, a furin recognition sequence SARNRQKR was incorporated downstream of the mouse Igκ light chain signal sequence (secretion signal peptide). The poly-histidine and c-myc tags were placed at the C terminus of the tF10 ORF. Assembled expression cassette including CMV promoter, hFX transgene open reading frame and the bovine growth hormone polyadenylation signal was ligated to a shuttle plasmid. Recombinant Ad genome was generated by homologous DNA recombination between shuttle plasmid and Ad5 genome backbone plasmid. Ad5tF10 was propagated in HEK293 cells, purified by cesium chloride gradient ultracentrifugation, and subjected to dialysis. To purify tF10 recombinant protein A549 cells were infected with Ad5tF10 vector at 50 $TCID_{50}$ per cell. Culture supernatants were collected for 7 days with media replacement and protein was precipitated using ammonium sulfate. Precipitate was collected by centrifugation, redissolved in PBS, and dialyzed against PBS. tF10 recombinant protein was purified by the immobilized metal-affinity chromatography (Ni-NTA Superflow, Qiagen). Eluted protein was dialyzed against PBS, filter-sterilized, and protein concentration was analyzed using the Lowry protein assay. Also, the conditioned media and purified protein were subjected to Western blot analysis using anti-myc and anti-His Abs.

For *in vivo* study AdH5RoboLuc and AdH5CMVLuc were incubated for 1 hour, either with tF10 or PBS and then mice were injected *via* the tail vein with 5×10^8 $TCID_{50}$ of recombinant Ad vectors. Three days after injection animals were humanely sacrificed by CO_2 inhalation, major organs were harvested and snap frozen in ethanol/dry ice mix and assessed for reporter gene expression using Luc assay described above. Lung-to-liver and spleen-to-liver ratios were calculated for each individual animal with the RLU normalized by the protein concentration of the tissue lysate and bars represent the mean ± s.d.

Quantitative RT-PCR assay

The levels of Robo4 mRNA expression were determined by reverse transcriptase PCR (RT-PCR). Total RNA was extracted from 1×10^7 cells using RNeasy Mini Kit (Qiagen), following standard protocol, and quantified specrophotometrically using a MBA 2000 spectrophotometer (Perkin Elmer, Wellesley, MA). cDNA was synthesized using random

hexamer primers and an Omniscript RT kit (Qiagen). The first-strand cDNA was used as the template for SYBP real-time PCR. For SYBP real-time PCR the following primers were used: Robo4-3162: 5′-CCGTCACTAGGCTTCTGGAG-3′; 3299-Robo4: 5′-TGGTTGTGGAGAGTCTGCTG-3′. After the initial denaturation (5 min at 95°C), amplification was performed with 40 cycles of 30 sec at 95°C, 20 sec at 62°C and 35 sec 72°C. Each sample was run in triplicate. The Robo4 gene specific qPCR template standard (OriGene Technologies, Rockville, MD) was used as an internal standard for template loading of PCR.

In vivo Ad hexon expression assay

Quantitative analysis of the Ad hexon gene expression was performed using real-time PCR. At 24 hours after intravenous injection with 5×10^8 $TCID_{50}$ of AdH5RoboLuc or AdH5/H3RoboLuc vectors, the animals were sacrificed and tissues were harvested and template DNA was prepared from whole tissue extracts using QIAamp DNA Mini Kit (Qiagen). For preparation of control samples, AdH5/H3RoboLuc genomic DNA was extracted from purified viral stock by using a QIAamp DNA Mini Kit. Serial 10-fold dilutions (from 1×10^7 to 1 viral particle per reaction) of AdH5/H3RoboLuc DNA were included in each run to establish a standard curve for quantitative appraisal of hexon target gene copy number. For detection of the Ad hexon gene, the following primers and TaqMan probe were used: Ad5hexon forward: 5′-TACGCACGACGTGACCACA-3′, Ad5hexon reverse: 5′-ATCCTCACGGTCCACAGGG-3′, and Ad5hexon probe: 5′-*6FAM*-ACCGGTCCCAGCGTTTGACGC-*BHQ1*-3′. The mouse β-actin gene was used as an internal standard for template loading of PCR by using primers: Actin forward: 5′-AGCTGGAGGACTTCCGAGACT-3′, Actin reverse: 5′-TGGCACTTCTCCTGCACCTT-3′, and Actin probe: 5′-*HEX*-TAGACGCCTGCACAAGCCGCC-*BHQ1*-3′.

In each reaction, 20 ng of total DNA was used as a template and PCR was performed in 25 μl of reaction mixture containing 12.5 μl of 2x TaqMan Universal PCR master Mix (PE Applied Biosystems, Foster City, CA), 300 nM of each primer, and 100 nM of fluorogenic probe. Amplifications were carried out in a 96-well reaction plate (PE Applied Biosystems) in a spectrofluorimetric thermal cycler (LightCycler® 480 System; Roche Applied Science, Indianapolis, IN). After the initial denaturation (2 min at 95°C), amplification was performed with 45 cycles of 15 sec at 95°C and 60 sec at 60°C. Each sample was run in triplicate. A threshold cycle (C_t) for each triplicate was estimated by determining the point at which the fluorescence exceeded a threshold limit (10-fold the standard deviation of the baseline). AdH5RoboLuc and AdH5/H3RoboLuc titers in different tissues were determined as the Ad hexon gene copy number per 1 ng total DNA.

Serum IL-6 cytokine and liver toxicity assay

Mice were injected intravenously with 5×10^8 $TCID_{50}$ of AdH5RoboLuc or AdH5/H3RoboLuc vectors, at 24 hours after injection the animals were sacrificed and sera were collected. The quantitative determination of the concentration of mouse IL-6 in serum was performed using the MaxDiscovery™ Mouse IL-6 ELISA Test Kit (Bioo Scientific, Austin, TX) and levels of enzymic activity of alanine aminotransferase (ALT) and aspartate aminotransferase (AST) were assayed with the MaxDiscovery™ enzymatic assay kit (Bioo Scientific) according to the manufacturer's protocol.

Statistical analysis

All error terms are expressed as the standard deviation of the mean. Significance levels for comparison of differences between groups in the *in vitro* experiments were analyzed by Student's *t* test. Differences were considered significant when *p*-values were < 0.05. In the

animal studies, the treatment groups were compared with respect to Luc expression in organs and lung-to-liver and spleen-to-liver ratio. To test for significant differences in mean Luc expression between treatment groups, one-way analysis of variance (ANOVA) test was conducted. Differences were considered significant when p-values were < 0.05.

Acknowledgments

The authors are grateful to William C. Aird and Yoshiaki Okada from the Center for Vascular Biology Research, Division of Molecular and Vascular Medicine, Beth Israel Deaconess Medical Center, Boston, MA, for providing the Robo4 promoter. The authors thank Dr. Hongju Wu from Tulane University, New Orleans, LA, and Dr. Andrew H. Baker from University of Glasgow, Glasgow, UK, for providing the pAd5/H3GL and pAd5*7* plasmids, respectively. This work was supported in part by National Heart, Lung and Blood Institute grant 5R01HL092941-02 and National Cancer Institute grant CA154697.

References

Aird WC. Endothelial cell heterogeneity. Crit Care Med. 2003; 31(4 Suppl):S221–30. [PubMed: 12682444]

Alba R, Bradshaw AC, Coughlan L, Denby L, McDonald RA, Waddington SN, Buckley SM, Greig JA, Parker AL, Miller AM, Wang H, Lieber A, van Rooijen N, McVey JH, Nicklin SA, Baker AH. Biodistribution and retargeting of FX-binding ablated adenovirus serotype 5 vectors. Blood. 2010; 116(15):2656–64. [PubMed: 20610817]

Alba R, Bradshaw AC, Parker AL, Bhella D, Waddington SN, Nicklin SA, van Rooijen N, Custers J, Goudsmit J, Barouch DH, McVey JH, Baker AH. Identification of coagulation factor (F)X binding sites on the adenovirus serotype 5 hexon: effect of mutagenesis on FX interactions and gene transfer. Blood. 2009; 114(5):965–71. [PubMed: 19429866]

Bachtarzi H, Stevenson M, Subr V, Ulbrich K, Seymour LW, Fisher KD. Targeting adenovirus gene delivery to activated tumour-associated vasculature via endothelial selectins. J Control Release. 2011; 150(2):196–203. [PubMed: 20965218]

Baker AH, Kritz A, Work LM, Nicklin SA. Cell-selective viral gene delivery vectors for the vasculature. Exp Physiol. 2005; 90(1):27–31. [PubMed: 15542621]

Bedell VM, Yeo SY, Park KW, Chung J, Seth P, Shivalingappa V, Zhao J, Obara T, Sukhatme VP, Drummond IA, Li DY, Ramchandran R. roundabout4 is essential for angiogenesis in vivo. Proceedings of the National Academy of Sciences of the United States of America. 2005; 102(18): 6373–8. [PubMed: 15849270]

Bergelson JM, Krithivas A, Celi L, Droguett G, Horwitz MS, Wickham T, Crowell RL, Finberg RW. The murine CAR homolog is a receptor for coxsackie B viruses and adenoviruses. Journal of virology. 1998; 72(1):415–9. [PubMed: 9420240]

Cefai D, Simeoni E, Ludunge KM, Driscoll R, von Segesser LK, Kappenberger L, Vassalli G. Multiply attenuated, self-inactivating lentiviral vectors efficiently transduce human coronary artery cells in vitro and rat arteries in vivo. Journal of molecular and cellular cardiology. 2005; 38(2):333–44. [PubMed: 15698840]

Dong Z, Nor JE. Transcriptional targeting of tumor endothelial cells for gene therapy. Adv Drug Deliv Rev. 2009; 61(7-8):542–53. [PubMed: 19393703]

Doronin K, Flatt JW, Di Paolo NC, Khare R, Kalyuzhniy O, Acchione M, Sumida JP, Ohto U, Shimizu T, Akashi-Takamura S, Miyake K, MacDonald JW, Bammler TK, Beyer RP, Farin FM, Stewart PL, Shayakhmetov DM. Coagulation factor X activates innate immunity to human species C adenovirus. Science. 2012; 338(6108):795–8. [PubMed: 23019612]

Edgar AJ, Chacon MR, Bishop AE, Yacoub MH, Polak JM. Upregulated genes in sporadic, idiopathic pulmonary arterial hypertension. Respiratory research. 2006; 7,

Everts M, Kim-Park SA, Preuss MA, Passineau MJ, Glasgow JN, Pereboev AV, Mahasreshti PJ, Grizzle WE, Reynolds PN, Curiel DT. Selective induction of tumor-associated antigens in murine pulmonary vasculature using double-targeted adenoviral vectors. Gene therapy. 2005; 12(13): 1042–8. [PubMed: 15789059]

Glasgow JN, Everts M, Curiel DT. Transductional targeting of adenovirus vectors for gene therapy. Cancer Gene Ther. 2006; 13(9):830–44. [PubMed: 16439993]

Gorn M, Anige M, Burkholder I, Muller B, Scheffler A, Edler L, Boeters I, Panse J, Schuch G, Hossfeld DK, Laack E. Serum levels of Magic Roundabout protein in patients with advanced non-small cell lung cancer (NSCLC). Lung cancer. 2005; 49(1):71–6. [PubMed: 15949592]

Greenberger S, Shaish A, Varda-Bloom N, Levanon K, Breitbart E, Goldberg I, Barshack I, Hodish I, Yaacov N, Bangio L, Goncharov T, Wallach D, Harats D. Transcription-controlled gene therapy against tumor angiogenesis. The Journal of clinical investigation. 2004; 113(7):1017–24. [PubMed: 15057308]

Grone J, Doebler O, Loddenkemper C, Hotz B, Buhr HJ, Bhargava S. Robo1/Robo4: differential expression of angiogenic markers in colorectal cancer. Oncology reports. 2006; 15(6):1437–43. [PubMed: 16685377]

He TC, Zhou S, da Costa LT, Yu J, Kinzler KW, Vogelstein B. A simplified system for generating recombinant adenoviruses. Proceedings of the National Academy of Sciences of the United States of America. 1998; 95(5):2509–14. [PubMed: 9482916]

Huminiecki L, Gorn M, Suchting S, Poulsom R, Bicknell R. Magic roundabout is a new member of the roundabout receptor family that is endothelial specific and expressed at sites of active angiogenesis. Genomics. 2002; 79(4):547–52. [PubMed: 11944987]

Jones CA, London NR, Chen H, Park KW, Sauvaget D, Stockton RA, Wythe JD, Suh W, Larrieu-Lahargue F, Mukouyama YS, Lindblom P, Seth P, Frias A, Nishiya N, Ginsberg MH, Gerhardt H, Zhang K, Li DY. Robo4 stabilizes the vascular network by inhibiting pathologic angiogenesis and endothelial hyperpermeability. Nature medicine. 2008; 14(4):448–53.

Jones CA, Nishiya N, London NR, Zhu W, Sorensen LK, Chan AC, Lim CJ, Chen H, Zhang Q, Schultz PG, Hayallah AM, Thomas KR, Famulok M, Zhang K, Ginsberg MH, Li DY. Slit2-Robo4 signalling promotes vascular stability by blocking Arf6 activity. Nature cell biology. 2009; 11(11): 1325–31.

Kalyuzhniy O, Di Paolo NC, Silvestry M, Hofherr SE, Barry MA, Stewart PL, Shayakhmetov DM. Adenovirus serotype 5 hexon is critical for virus infection of hepatocytes in vivo. Proc Natl Acad Sci U S A. 2008; 105(14):5483–8. [PubMed: 18391209]

Kaur S, Castellone MD, Bedell VM, Konar M, Gutkind JS, Ramchandran R. Robo4 signaling in endothelial cells implies attraction guidance mechanisms. The Journal of biological chemistry. 2006; 281(16):11347–56. [PubMed: 16481322]

Kim J, Nam HY, Kim TI, Kim PH, Ryu J, Yun CO, Kim SW. Active targeting of RGD-conjugated bioreducible polymer for delivery of oncolytic adenovirus expressing shRNA against IL-8 mRNA. Biomaterials. 2011; 32(22):5158–66. [PubMed: 21531456]

Koch AW, Mathivet T, Larrivee B, Tong RK, Kowalski J, Pibouin-Fragner L, Bouvree K, Stawicki S, Nicholes K, Rathore N, Scales SJ, Luis E, del Toro R, Freitas C, Breant C, Michaud A, Corvol P, Thomas JL, Wu Y, Peale F, Watts RJ, Tessier-Lavigne M, Bagri A, Eichmann A. Robo4 maintains vessel integrity and inhibits angiogenesis by interacting with UNC5B. Developmental cell. 2011; 20(1):33–46. [PubMed: 21238923]

Koski A, Rajecki M, Guse K, Kanerva A, Ristimaki A, Pesonen S, Escutenaire S, Hemminki A. Systemic adenoviral gene delivery to orthotopic murine breast tumors with ablation of coagulation factors, thrombocytes and Kupffer cells. J Gene Med. 2009; 11(11):966–77. [PubMed: 19670332]

Legg JA, Herbert JM, Clissold P, Bicknell R. Slits and Roundabouts in cancer, tumour angiogenesis and endothelial cell migration. Angiogenesis. 2008; 11(1):13–21. [PubMed: 18264786]

Marlow R, Binnewies M, Sorensen LK, Monica SD, Strickland P, Forsberg EC, Li DY, Hinck L. Vascular Robo4 restricts proangiogenic VEGF signaling in breast. Proceedings of the National Academy of Sciences of the United States of America. 2010; 107(23):10520–5. [PubMed: 20498081]

Okada Y, Yano K, Jin E, Funahashi N, Kitayama M, Doi T, Spokes K, Beeler DL, Shih SC, Okada H, Danilov TA, Maynard E, Minami T, Oettgen P, Aird WC. A three-kilobase fragment of the human Robo4 promoter directs cell type-specific expression in endothelium. Circulation research. 2007; 100(12):1712–22. [PubMed: 17495228]

Park KW, Morrison CM, Sorensen LK, Jones CA, Rao Y, Chien CB, Wu JY, Urness LD, Li DY. Robo4 is a vascular-specific receptor that inhibits endothelial migration. Developmental biology. 2003; 261(1):251–67. [PubMed: 12941633]

Parker AL, McVey JH, Doctor JH, Lopez-Franco O, Waddington SN, Havenga MJ, Nicklin SA, Baker AH. Influence of coagulation factor zymogens on the infectivity of adenoviruses pseudotyped with fibers from subgroup D. Journal of virology. 2007; 81(7):3627–31. [PubMed: 17251290]

Parker AL, Waddington SN, Nicol CG, Shayakhmetov DM, Buckley SM, Denby L, Kemball-Cook G, Ni S, Lieber A, McVey JH, Nicklin SA, Baker AH. Multiple vitamin K-dependent coagulation zymogens promote adenovirus-mediated gene delivery to hepatocytes. Blood. 2006; 108(8):2554–61. [PubMed: 16788098]

Preuss MA, Glasgow JN, Everts M, Stoff-Khalili MA, Wu H, Curiel DT. Enhanced Gene Delivery to Human Primary Endothelial Cells Using Tropism-Modified Adenovirus Vectors. Open Gene Ther J. 2008; 1,:7–11. [PubMed: 19834585]

Reynolds PN, Nicklin SA, Kaliberova L, Boatman BG, Grizzle WE, Balyasnikova IV, Baker AH, Danilov SM, Curiel DT. Combined transductional and transcriptional targeting improves the specificity of transgene expression in vivo. Nature biotechnology. 2001; 19(9):838–42.

Savontaus MJ, Sauter BV, Huang TG, Woo SL. Transcriptional targeting of conditionally replicating adenovirus to dividing endothelial cells. Gene therapy. 2002; 9(14):972–9. [PubMed: 12085246]

Seth P, Lin Y, Hanai J, Shivalingappa V, Duyao MP, Sukhatme VP. Magic roundabout, a tumor endothelial marker: expression and signaling. Biochemical and biophysical research communications. 2005; 332(2):533–41. [PubMed: 15894287]

Sharma A, Bangari DS, Tandon M, Hogenesch H, Mittal SK. Evaluation of innate immunity and vector toxicity following inoculation of bovine, porcine or human adenoviral vectors in a mouse model. Virus research. 2010; 153(1):134–42. [PubMed: 20659505]

Shashkova EV, Doronin K, Senac JS, Barry MA. Macrophage depletion combined with anticoagulant therapy increases therapeutic window of systemic treatment with oncolytic adenovirus. Cancer research. 2008; 68(14):5896–904. [PubMed: 18632644]

Shayakhmetov DM, Gaggar A, Ni S, Li ZY, Lieber A. Adenovirus binding to blood factors results in liver cell infection and hepatotoxicity. Journal of virology. 2005; 79(12):7478–91. [PubMed: 15919903]

Shinozaki K, Suominen E, Carrick F, Sauter B, Kahari VM, Lieber A, Woo SL, Savontaus M. Efficient infection of tumor endothelial cells by a capsid-modified adenovirus. Gene Ther. 2006; 13(1):52–9. [PubMed: 16107861]

Short JJ, Rivera AA, Wu H, Walter MR, Yamamoto M, Mathis JM, Curiel DT. Substitution of adenovirus serotype 3 hexon onto a serotype 5 oncolytic adenovirus reduces factor X binding, decreases liver tropism, and improves antitumor efficacy. Molecular cancer therapeutics. 2010; 9(9):2536–44. [PubMed: 20736345]

Smith-Berdan S, Nguyen A, Hassanein D, Zimmer M, Ugarte F, Ciriza J, Li D, Garcia-Ojeda ME, Hinck L, Forsberg EC. Robo4 cooperates with CXCR4 to specify hematopoietic stem cell localization to bone marrow niches. Cell Stem Cell. 2011; 8(1):72–83. [PubMed: 21211783]

Song W, Sun Q, Dong Z, Spencer DM, Nunez G, Nor JE. Antiangiogenic gene therapy: disruption of neovascular networks mediated by inducible caspase-9 delivered with a transcriptionally targeted adenoviral vector. Gene therapy. 2005; 12(4):320–9. [PubMed: 15616606]

Takayama K, Reynolds PN, Adachi Y, Kaliberova L, Uchino J, Nakanishi Y, Curiel DT. Vascular endothelial growth factor promoter-based conditionally replicative adenoviruses for pan-carcinoma application. Cancer gene therapy. 2007; 14(1):105–16. [PubMed: 17024232]

Tallone T, Malin S, Samuelsson A, Wilbertz J, Miyahara M, Okamoto K, Poellinger L, Philipson L, Pettersson S. A mouse model for adenovirus gene delivery. Proceedings of the National Academy of Sciences of the United States of America. 2001; 98(14):7910–5. [PubMed: 11438737]

Waddington SN, McVey JH, Bhella D, Parker AL, Barker K, Atoda H, Pink R, Buckley SM, Greig JA, Denby L, Custers J, Morita T, Francischetti IM, Monteiro RQ, Barouch DH, van Rooijen N, Napoli C, Havenga MJ, Nicklin SA, Baker AH. Adenovirus serotype 5 hexon mediates liver gene transfer. Cell. 2008; 132(3):397–409. [PubMed: 18267072]

Wickham TJ, Mathias P, Cheresh DA, Nemerow GR. Integrins alpha v beta 3and alpha v beta 5 promote adenovirus internalization but not virus attachment. Cell. 1993; 73(2):309–19. [PubMed: 8477447]

Work LM, Buning H, Hunt E, Nicklin SA, Denby L, Britton N, Leike K, Odenthal M, Drebber U, Hallek M, Baker AH. Vascular bed-targeted in vivo gene delivery using tropism-modified adeno-associated viruses. Mol Ther. 2006; 13(4):683–93. [PubMed: 16387552]

Wu H, Dmitriev I, Kashentseva E, Seki T, Wang M, Curiel DT. Construction and characterization of adenovirus serotype 5 packaged by serotype 3 hexon. Journal of virology. 2002; 76(24):12775–82. [PubMed: 12438602]

Wung BS, Ni CW, Wang DL. ICAM-1 induction by TNFalpha and IL-6 is mediated by distinct pathways via Rac in endothelial cells. Journal of biomedical science. 2005; 12(1):91–101. [PubMed: 15864742]

Xu Z, Qiu Q, Tian J, Smith JS, Conenello GM, Morita T, Byrnes AP. Coagulation factor X shields adenovirus type 5 from attack by natural antibodies and complement. Nature medicine. 2013; 19(4):452–7.

Yang WY, Huang ZH, Lin LJ, Li Z, Yu JL, Song HJ, Qian Y, Che XY. Kinase domain insert containing receptor promoter controlled suicide gene system selectively kills human umbilical vein endothelial cells. World journal of gastroenterology : WJG. 2006; 12(33):5331–5. [PubMed: 16981263]

Zhang X, Yu J, Kuzontkoski PM, Zhu W, Li DY, Groopman JE. Slit2/Robo4 signaling modulates HIV-1 gp120-induced lymphatic hyperpermeability. PLoS Pathog. 2012; 8(1):e1002461. [PubMed: 22241990]

Zhuang X, Cross D, Heath VL, Bicknell R. Shear stress, tip cells and regulators of endothelial migration. Biochemical Society transactions. 2011; 39(6):1571–5. [PubMed: 22103489]

Zinn KR, Szalai AJ, Stargel A, Krasnykh V, Chaudhuri TR. Bioluminescence imaging reveals a significant role for complement in liver transduction following intravenous delivery of adenovirus. Gene therapy. 2004; 11(19):1482–6. [PubMed: 15295616]

Highlights

- Robo4 promoter was used for Ad5 endothelium targeting and liver untargeting.
- We demonstrate the utility of the Robo4 promoter in an Ad5 vector context.
- Substitution of the Ad5 hexon with the HVR7 from Ad3 decreased liver sequestration.
- Double targeting approach improved the biodistribution of Ad5 gene expression.

A

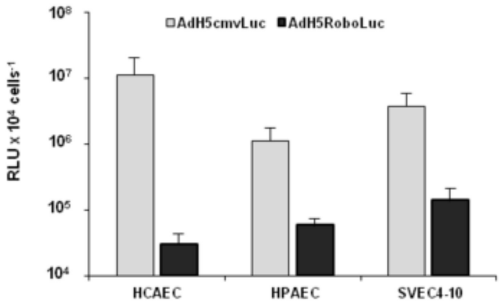

B

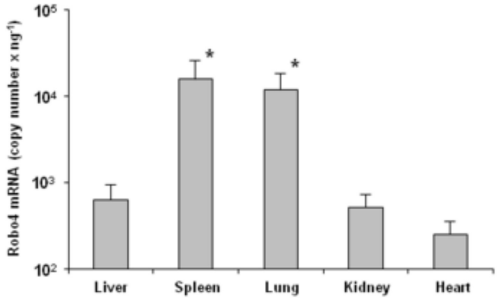

C

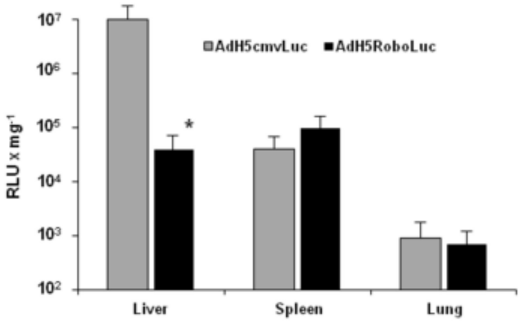

D

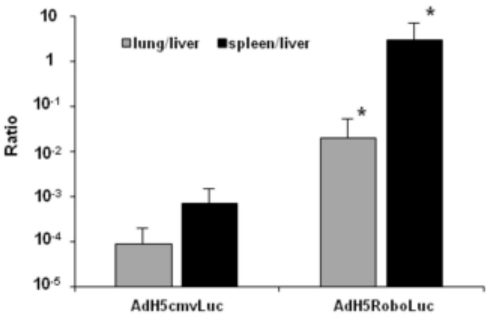

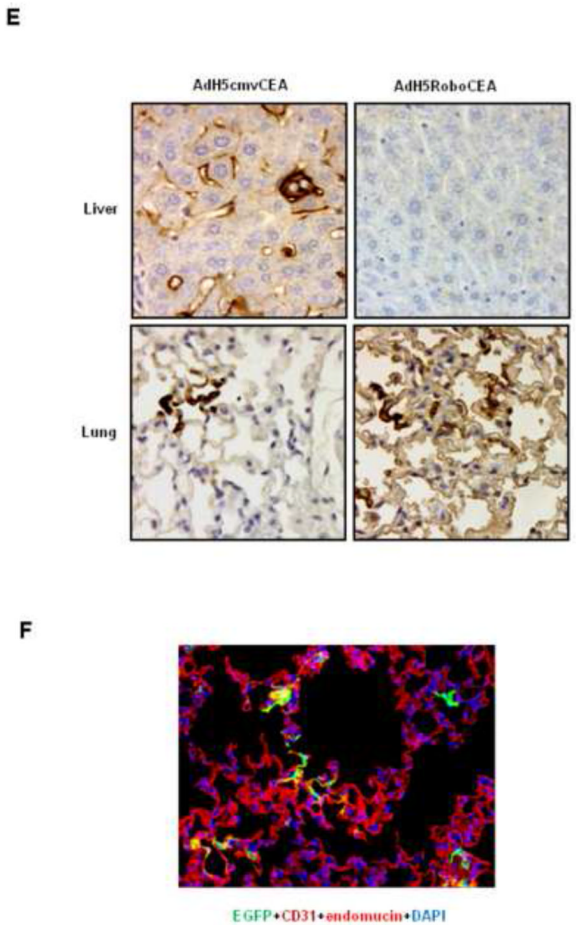

Fig. 1. Characterization of recombinant Ad vectors containing the Robo4 endothelial-specific promoter.

(**A**) Characterization of the Robo4 endothelial-specific promoter in vitro. The human Robo4 promoter was utilized for transcriptional targeting of Ad mediated Luc expression. Infection of human and murine endothelial cells with AdH5RoboLuc yielded in variable levels of Luc expression which were relatively low compared to AdH5CMVLuc. Each bar represents the mean relative light units (RLU) per cell (n=6) ± s.d. (**B**) Robo4 mRNA expression in vivo. Murine organs were collected and Robo4 mRNA expression was assessed by quantitative RT-PCR analysis. Lung and spleen demonstrated high levels of Robo4 mRNA expression in comparison with liver. Kidney and heart showed the lowest levels of Robo4 mRNA expression between tested tissues (*, $P < 0.05$ vs Liver). (**C**) Ad mediated Luc expression *in vivo*. Luc activity was measured in major organs at 3 days after systemic administration of AdH5RoboLuc or AdH5CMVLuc. Luc expression was observed mainly in the liver and spleen and relatively low expression observed in the lung following *i.v.* injection of AdH5CMVLuc vector. Systemic administration of AdH5RoboLuc produced Luc expression in the liver that was significantly lower than AdH5CMVLuc. Each bar represents the mean RLU per mg total protein ± s.d. (*, $P < 0.01$ vs AdH5cmvLuc). (**D**) Ad targeting efficiency. The lung-to-liver and the spleen-to-liver ratio of Luc expression were significantly increased after systemic administration of AdH5RoboLuc in comparison with AdH5CMVLuc (*, $P < 0.01$ vs AdH5cmvLuc). (**E**) Immunohistochemical analysis of CEA expression. Photomicrographs of immunocytochemistry staining of liver and spleen sections from hCAR transgenic mice stained with an anti-CEA antibody. Representative areas of lung (lower panels) and liver (upper panels) from an animal treated with AdH5CMVCEA (left

panels) or AdH5RoboCEA (right panels). Original magnification was ×600 for all panels. Employment of the Robo4 promoter results in decreased CEA expression in the liver. Liver expression is only observed for AdH5CMVCEA, while the vasculature of the lung of hCAR transgenic mice efficiently expresses CEA after AdH5RoboCEA injection. Immunostaining with CEA revealed that Robo4 promoter activity was localized in the lung capillary endothelium, while promoter activity was undetectable in hepatocytes and Kupffer cells. (**F**) Co-immunofluorescence analysis of EGFP reporter gene expression. hCAR transgenic mice were injected with AdH5RoboEGFP. Two days post injection mouse lungs were collected and immunofluorescent localization of EGFP protein expression was analyzed. EGFP expression in lung tissue was co-localized with CD31 and endomucin.

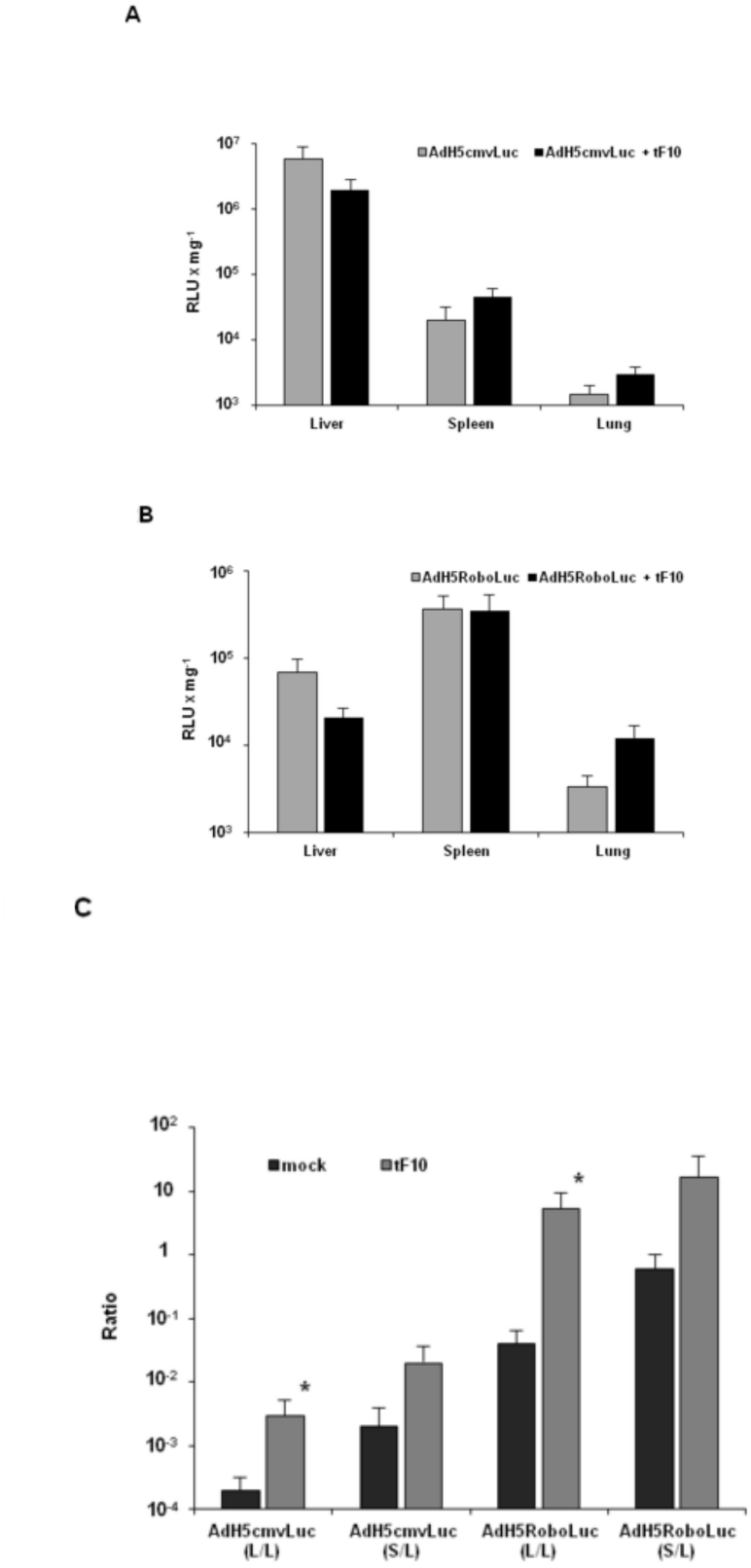

Fig. 2. Blocking of binding of FX with Ad5 hexon decrease liver uptake

AdH5CMVLuc (**A**) and AdH5RoboLuc (**B**) were incubated with tF10 or PBS and then mice were injected *via* the tail vein with 5×10^8 $TCID_{50}$ of recombinant Ad vectors. Three days after injection animals were humanely sacrificed, major organs were harvested and assessed for reporter gene expression using Luc assay. Preincubation of AdH5CMVLuc and AdH5RoboLuc with truncated form of hFX resulted in decreased transgene expression in liver and increased Luc expression in lung. Each bar represents the mean RLU per mg total protein ± s.d. (**C**) The lung-to-liver (L/L) and spleen-to-liver (S/L) ratios of Luc expression were increased in mice following *i.v.* injection with AdH5CMVLuc and AdH5RoboLuc incubated with tF10 in comparison with mock-treated Ads. Data points represent the mean ± s.d. of a representative experiment (*, $P < 0.05$ vs no tF10 treatment).

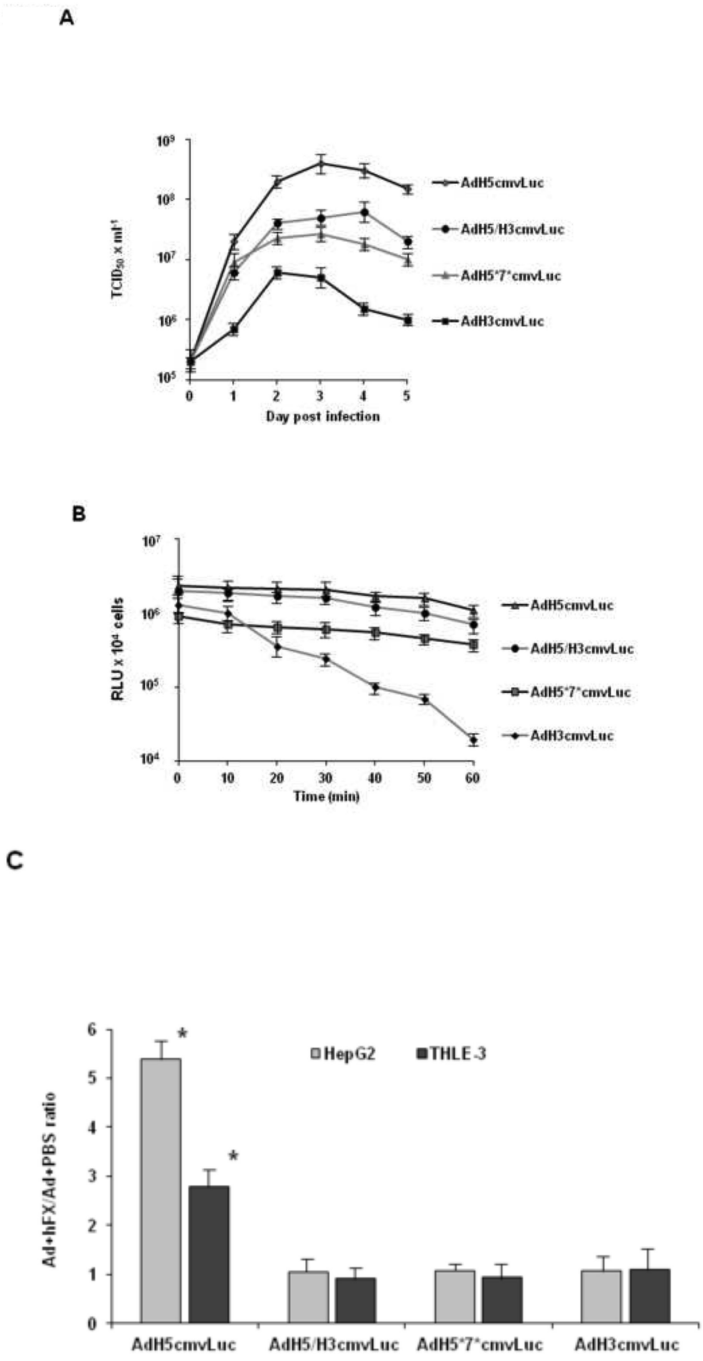

Fig. 3. In vitro characterization of recombinant Ads

(**A**) Growth kinetics of hexon-modified Ad vectors. HEK293 cells were infected with Ad vectors at 5 $TCID_{50}$ $cell^{-1}$. Cells and culture medium were harvested at different time after infection. The viral titers were determined by $TCID_{50}$ assay. (**B**). Thermostability of recombinant Ad vectors. The viruses were incubated at 42°C for different time intervals before the infection of A549 cells. Forty-eight h after infection cells were subjected to Luc assay. (**C**) Gene transfer assay. Recombinant Ads were incubated with hFX or PBS and then HepG2 and THLE-3 cells were infected with Ad vectors at 5 $TCID_{50}$ $cell^{-1}$ and cell lysates

were analyzed for Luc activity. Data are means ± s.d. of a representative experiment with triplicate samples (*, $P < 0.05$ vs no hFX treatment)

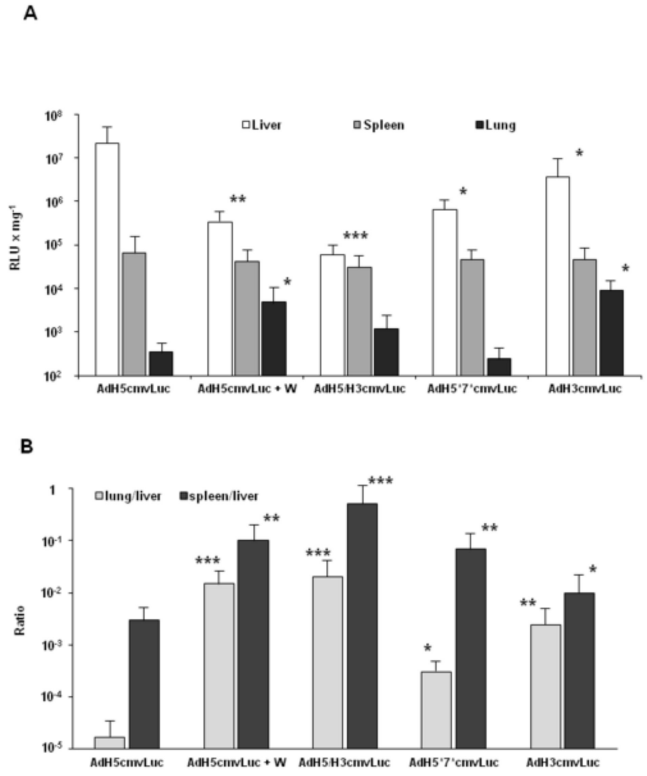

Fig. 4. Biodistribution of transgene expression in vivo

(**A**) Ads with hexon modifications demonstrate reduced liver transduction *in vivo* following systemic administration. Female C57BL6J mice (5-7 weeks old, n=5 per group) were injected through the tail vein with 5×10^8 $TCID_{50}$ of AdH5/H3CMVLuc, AdH5*7*CMVLuc or AdH3CMVLuc vectors or AdH5CMVLuc alone or following pretreatment with warfarin (AdH5CMVLuc + W). Three days after injection animals were humanely sacrificed, major organs were harvested and snap frozen in ethanol/dry ice mix and assessed for reporter gene expression using Luc assay. (**B**) The lung-to-liver and spleen-to-liver ratios were significantly increased in mice following *i.v*. injection with hexon-modified Ads and after pretreatment warfarin in comparison with wild-type hexon AdH5CMVLuc alone. Data are means ± s.d. (*, $P < 0.05$; **, $P < 0.01$; ***, $P < 0.001$ vs AdH5cmvLuc).

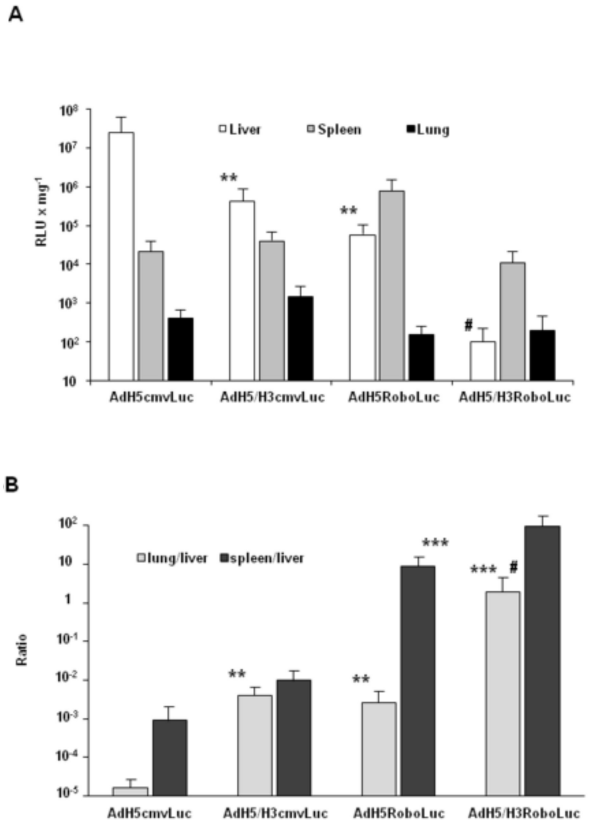

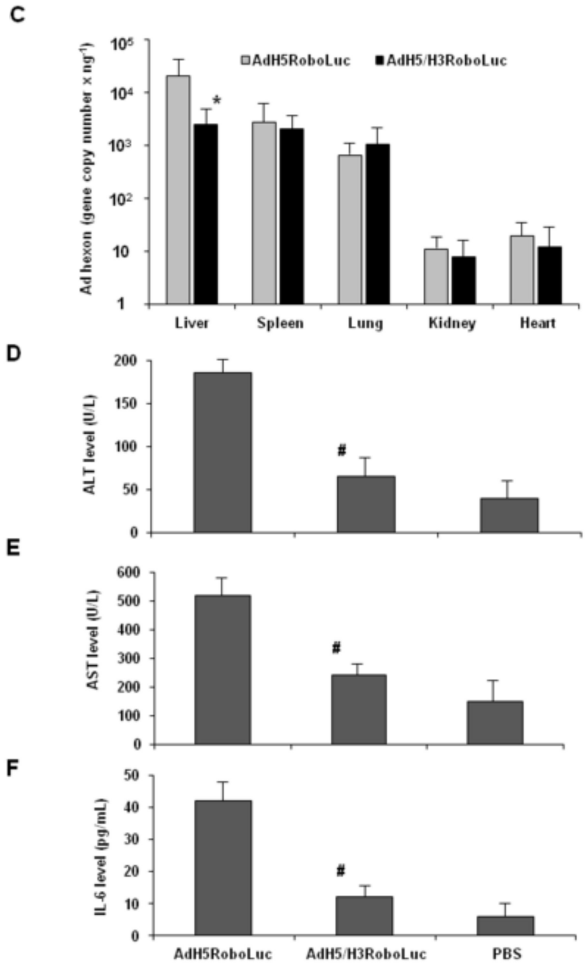

Fig. 5. Biodistribution of Robo4-driven transgene expression in vivo

(**A**) Hexon-modified AdH5/H3RoboLuc demonstrates reduced liver transduction *in vivo* following systemic administration. Female C57BL6J mice (5-7 weeks old, n=5 per group) were injected through the tail vein with 5×10^8 $TCID_{50}$ of AdH5CMVLuc, AdH5/H3CMVLuc, AdH5RoboLuc or AdH5/H3RoboLuc vectors. Three days after injection animals were humanely sacrificed, livers, spleens and lungs were harvested and snap frozen in ethanol/dry ice mix and assessed for reporter gene expression using Luc assay. (**B**) The lung-to-liver and spleen-to-liver ratios of Luc expression were significantly increased in mice following *i.v.* injection with AdH5/H3RoboLuc in comparison with other tested Ads. Data points represent the mean ± s.d. of a representative experiment. (**C**) Distribution of Ad viral particles *in vivo*. Mice were *i.v.* injected with 5×10^8 $TCID_{50}$ of AdH5RoboLuc or AdH5/H3RoboLuc and major organs were collected at 24 hours after Ad vectors administration. Quantitative analysis of the Ad hexon gene expression was performed using TaqMan PCR. For analysis of enzymic activity of ALT (**D**) and AST (**E**) C57BL6 mice were injected with AdH5RoboLuc or AdH5/H3RoboLuc vectors. Twenty-four hours post Ad injection sera were collected and levels of ALT and AST were measured. (**F**) Quantitative determination of the IL-6 expression. Analysis of IL-6 levels in mouse serum following single *i.v.* injection with AdH5RoboLuc or AdH5/H3RoboLuc. Data are means ± s.d. for 5 mice per group (*, $P < 0.05$; **, $P < 0.01$; ***, $P < 0.001$ vs AdH5cmvLuc; #, $P < 0.05$ vs AdH5RoboLuc).

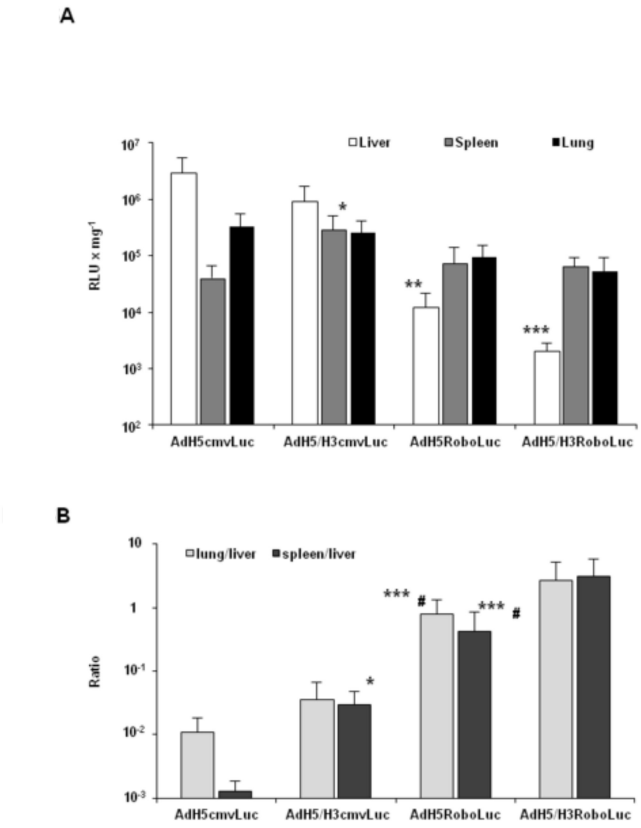

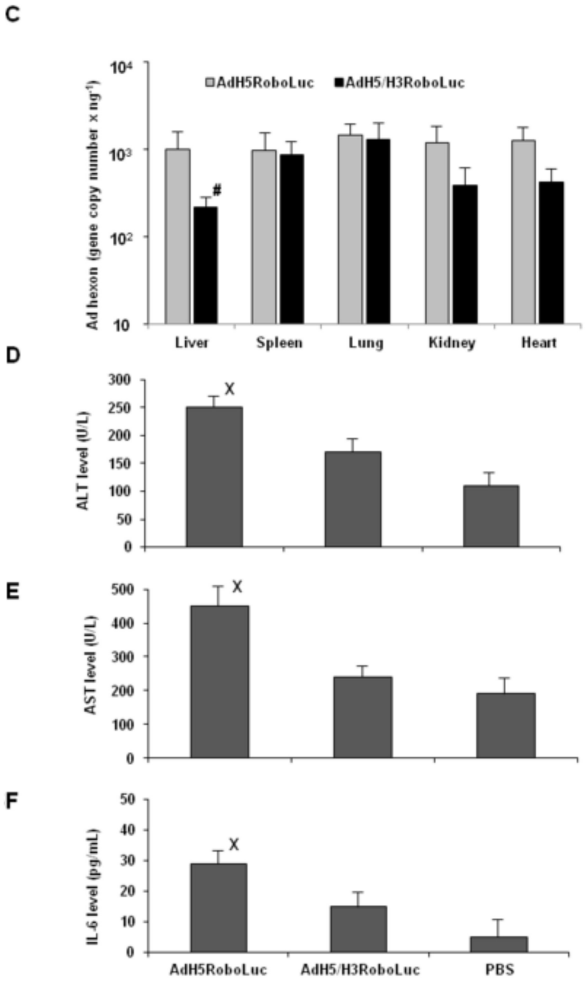

Fig. 6. Biodistribution of gene expression in hCAR transgenic mice

(**A**) AdH5RoboLuc or AdH5/H3RoboLuc vectors demonstrate reduced liver transduction *in vivo* following systemic administration. The transgenic female hCAR mice were injected through the tail vein with 5×10^8 $TCID_{50}$ of AdH5CMVLuc, AdH5/H3CMVLuc, AdH5RoboLuc or AdH5/H3RoboLuc. Three days after injection liver, spleen and lung were snap frozen and Luc levels quantified. (**B**) The lung-to-liver and spleen-to-liver ratios were significantly increased in mice following *i.v.* injection with AdH5RoboLuc or AdH5/H3RoboLuc in comparison with wild-type hexon AdH5CMVLuc and hexon-modified AdH5/H3CMVLuc. Data are means ± s.d. of a representative experiment. (**C**) Distribution of Ad viral particles *in vivo*. Mice were *i.v.* injected with 5×10^8 $TCID_{50}$ of AdH5RoboLuc or AdH5/H3RoboLuc (5 mice per group), major organs were collected at 24 hours after Ad vectors administration. Quantitative analysis of the Ad hexon gene expression was performed using TaqMan PCR. Serum levels of ALT (**D**) and AST (**E**) in hCAR mice. Twenty-four hours after AdH5RoboLuc or AdH5/H3RoboLuc administration sera were collected and levels of ALT and AST enzymic activity were evaluated. (**F**) Analysis of serum levels of IL-6. Quantitative determination of serum IL-6 in mice after intravenous injection with AdH5RoboLuc or AdH5/H3RoboLuc was performed using ELISA. Data are means ± s.d. (*, $P < 0.05$; **, $P < 0.01$; ***, $P < 0.001$ vs AdH5cmvLuc; +, $P < 0.05$ vs AdH5RoboLuc; X, $P < 0.05$ vs PBS).

Table 1

Recombinant Ad vectors used in this study.

Virus [a]	Promoter [b]	Transgene [c]	Hexon [d]
AdH5cmvLuc	CMV	Luc	H5
AdH5RoboLuc	Robo4	Luc	H5
AdH5cmvCEA	CMV	CEA	H5
AdH5RoboCEA	Robo4	CEA	H5
AdH5RoboEGFP	Robo4	EGFP	H5
AdH5/H3RoboLuc	Robo4	Luc	H5/H3
AdH5/H3cmvLuc	CMV	Luc	H5/H3
AdH5*7*cmvLuc	CMV	Luc	H5*7*
AdH3cmvLuc	CMV	Luc	H3

[a] Genomic regions relevant to our proposed studies are shown.

[b] CMV, human cytomegalovirus enhancer/promoter; Robo4, Roundabout 4 receptor enhancer/promoter.

[c] Luc, firefly luciferase; CEA, carcinoembryonic antigen; EGFP, enhanced green fluorescent protein.

[d] H5, wild-type Ad serotype 5 hexon; H5/H3, Ad5 hexon with substitution the hypervariable region 7 (HVR7) from Ad serotype 3; H5*7*, Ad5 hexon with point mutations within HVR5 (T270P and E271G) and HVR7 (I421G, T423N, E424S, L426Y, and E451Q); H3, Ad3 hexon swapping.